

Physiological Adaptation of the Bacterium *Lactococcus lactis* in Response to the Production of Human CFTR*[§]

Anton Steen[‡], Elena Wiederhold^{‡§§}, Tejas Gandhi^{‡§}, Rainer Breitling^{§**}, and Dirk Jan Slotboom^{‡¶}

Biochemical and biophysical characterization of CFTR (the cystic fibrosis transmembrane conductance regulator) is thwarted by difficulties to obtain sufficient quantities of correctly folded and functional protein. Here we have produced human CFTR in the prokaryotic expression host *Lactococcus lactis*. The full-length protein was detected in the membrane of the bacterium, but the yields were too low (< 0.1% of membrane proteins) for *in vitro* functional and structural characterization, and induction of the expression of CFTR resulted in growth arrest. We used isobaric tagging for relative and absolute quantitation based quantitative proteomics to find out why production of CFTR in *L. lactis* was problematic. Protein abundances in membrane and soluble fractions were monitored as a function of induction time, both in CFTR expression cells and in control cells that did not express CFTR. Eight hundred and forty six proteins were identified and quantified (35% of the predicted proteome), including 163 integral membrane proteins. Expression of CFTR resulted in an increase in abundance of stress-related proteins (e.g. heat-shock and cell envelope stress), indicating the presence of misfolded proteins in the membrane. In contrast to the reported consequences of membrane protein overexpression in *Escherichia coli*, there were no indications that the membrane protein insertion machinery (Sec) became overloaded upon CFTR production in *L. lactis*. Nutrients and ATP became limiting in the control cells as the culture entered the late exponential and stationary growth phases but this did not happen in the CFTR expressing cells, which had stopped growing upon induction. The different stress responses elicited in *E. coli* and *L. lactis* upon membrane protein production indicate that

different strategies are needed to overcome low expression yields and toxicity. *Molecular & Cellular Proteomics* 10: 10.1074/mcp.M000052-MCP200, 1–16, 2011.

The human cystic fibrosis transmembrane conductance regulator CFTR¹ is an atypical member of the superfamily of ATP binding cassette (ABC) transporters, because it is a channel (for chloride ions) rather than a transporter. Mutations in CFTR cause cystic fibrosis (1–3), the most common genetic disease among Caucasians. Mechanistic studies on CFTR and attempts to rationally design drugs to treat cystic fibrosis are hampered by difficulties to produce the protein in amounts needed for biochemical and biophysical studies, such as x-ray crystallography. A major bottleneck is a lack of suitable overexpression systems to produce recombinant CFTR, a problem which is often encountered for human membrane proteins (4–11). In an attempt to find suitable hosts for recombinant production of CFTR the cystic fibrosis foundation has funded a project to express CFTR in the bacterium *Lactococcus lactis*.

L. lactis is a Gram-positive bacterium for which expression plasmids and inducible promoters are available (12). Several cases have been reported in which functional overexpression of membrane proteins could be achieved in *L. lactis*, but not in *E. coli* (e.g. the human KDEL receptor, Na⁺/tyrosine transporter (Tyt1) of *Fusobacterium nucleatum* and several membrane proteins from *Arabidopsis*) (5, 13–17). The use of *L. lactis* as host for (eukaryotic) membrane protein expression has been reviewed by Kunji *et al.* (14). Among the potential advantages of *L. lactis* are its growth rate of ~1 doubling per hour, which is much slower than *E. coli* and could be beneficial for expression of proteins that do not fold easily. Also the presence of a different repertoire of chaperones, e.g. two copies of the integral membrane

From the [‡]Department of Biochemistry Groningen Biomolecular Sciences and Biotechnology Institute, University of Groningen, Nijenborgh 4, 9747 AG, Groningen, The Netherlands; [§]Groningen Bioinformatics Centre, Groningen Biomolecular Sciences and Biotechnology Institute, University of Groningen, Nijenborgh 7 9747 AG Groningen The Netherlands; ^{§§}Institute for Plant Biology University of Zurich Zollikerstrasse 107 8008 Zurich Switzerland; ^{**}Institute of Molecular, Cell and Systems Biology College of Medical, Veterinary and Life Sciences Joseph Black Building B3.10 University of Glasgow Glasgow G12 8QQ United Kingdom

Received and accepted on April 26, 2010

Published, MCP Papers in Press, April 26, 2010, DOI: 10.1074/mcp.M000052-MCP200

¹ The abbreviations used are: CFTR, cystic fibrosis transmembrane conductance regulator; DDM, *n*-dodecyl- β -D-maltoside; iTRAQ, isobaric tag for relative and absolute quantification; MALDI, matrix assisted laser desorption/ionisation; MBP, maltose binding protein; MMTS, methyl methanethiosulfonate; PMSF, phenyl methanesulphonyl fluoride; TEAB, triethylammonium bicarbonate buffer; TFA, trifluoroacetic acid; TOF, time-of-flight.

chaperone YidC (18–20), could facilitate insertion and assembly of heterologous membrane proteins. Other factors such as different membrane lipids and cytosolic environment could play a role as well.

Here we have used *L. lactis* for the expression of the human cystic fibrosis transmembrane conductance regulator CFTR. We were able to express full length (1480 amino acids long) CFTR in the bacterial host, but the expression levels were too low for to pursue structural studies, and expression was toxic to the cells. To understand this toxicity and to identify potential remedies to improve expression levels, we investigated the physiological responses that were elicited in *L. lactis* upon CFTR expression by performing a global quantitative proteomics study.

EXPERIMENTAL PROCEDURES

DNA Manipulations and Cloning of CFTR—Human *cftr* cDNA (gift from Christine Bear, Toronto) (accession nr M28668) was cloned into the *E. coli* vectors pREnLIC, and pREcLIC (supplemental Table 1), which introduce the sequences coding for N- and C-terminal His₁₀-tags, respectively, by Ligation Independent Cloning (LIC) as described by Geertsma *et al.* (21), yielding plasmids pREnCFTR and pREcCFTR. Plasmid pREnCFTR, which contains the *cftr* coding region fused to sequences coding for both an N- and C-terminal His₁₀-tag, was constructed by exchanging the NcoI-XhoI fragment of pREnCFTR with the NcoI-XhoI fragment of pREcCFTR. pRE_MBP-CFTR was constructed by amplifying *cftr* by PCR and subsequent cloning in the NcoI and SpeI sites of pRE_MBP (supplemental Table 1). The pRE vectors were converted into pNZ8048-related vectors for *L. lactis* by Vector Backbone Exchange as described by Geertsma *et al.* (21).

Expression of CFTR in *L. lactis* and Sample Preparation—*L. lactis* NZ9000 transformed with pNZ8048-derived plasmids was cultivated in M17 medium (Oxoid, Basingstoke, UK) containing 1% glucose, and 5 µg/ml chloramphenicol. To test for expression of CFTR *L. lactis* was grown in 10-ml cultures (inoculated with O/N cultures that were diluted 1:50) to an OD₆₀₀ of 0.5 at 30 °C, after which Nisin A (1:5000 dilution of the culture supernatant of the nisin producing strain *L. lactis* NZ9700 (5)) was added and the cells were incubated for another 2 h. A volume of culture containing the equivalent amount of cells as 1 ml of OD₆₀₀ of 5 was spun down (20,000 × *g*, 2 min, room temperature) and the pellet was resuspended in 400 µl of 50 mM potassium phosphate buffer (KP_i) pH 7.5, 10% glycerol. Phenyl methanesulphonyl fluoride (1 mM) was added and the cells were disrupted in a Fastprep machine (Bio101, Vista, CA) by vigorous shaking in the presence of glass beads (two times at force 6.0 for 30 s, with 10 min incubation on ice in between the two runs). The crude cell extracts were supplemented with EDTA (15 mM final concentration) and centrifuged for 15 min at 20,000 × *g* at 4 °C. The supernatant was subsequently centrifuged at 300,000 × *g* (30 min, 4 °C) to obtain the membranes.

SDS-sample buffer was added and samples were incubated at 37 °C for 5 min before loading on SDS-PAGE. His-tag specific antibodies (GE healthcare) and CFTR C terminus specific antibodies (clone 24–1, R&D systems) were used for western hybridizations.

Purification of His-MBP-CFTR—*L. lactis* NZ9000 pNZ_MBP-CFTR was grown in a fermenter (Applikon) in 2 L M17 supplemented with glucose (1%) and chloramphenicol (5 µg/ml) as described later. The cells were harvested 2 h after induction by centrifugation (6800 × *g*, 15 min, 4 °C) and membranes were prepared as described later. The membranes were stored at –80 °C in 50 mM KP_i pH 7.5, 10% glycerol at a concentration of 10 mg/ml protein.

Membranes containing 10 mg protein were resuspended in 10 ml of 50 mM Tris-HCl pH 8.0, 300 mM NaCl, 20% glycerol, 10 mM Imidazole. n-Dodecyl-β-D-maltoside (DDM) was added (1% final concentration) and the proteins were solubilized on ice for 1 h. Solubilized membranes were centrifuged at 100,000 × *g* for 30 min at 4 °C. The supernatant was incubated with Ni-Sepharose resin (GE Healthcare) for 1 h (400 µl slurry, which had been pre-equilibrated with solubilization buffer), with gentle rotation. The resin was washed with 10 ml of the same buffer containing 0.05% DDM and 50 mM imidazole and finally proteins were eluted with buffer containing 500 mM imidazole and 0.05% DDM (100, 200, 200 µl fractions).

In-gel Trypsin Digest—Bands were excised from a Coomassie Blue-stained SDS-PAGE and cut into ~1 mm³ pieces. Gel slices were incubated 3–4 times for 15 min in 150 µl of destaining solution (50% acetonitrile, 50 mM ammonium bicarbonate). The gel slices were dehydrated in 150 µl of 100% acetonitrile for 10 min, the supernatant was discarded and the gel slices were dried by evaporation. The reduction of cysteine residues was performed by incubating the gel slices in 30 µl of 10 mM dithiothreitol in 50 mM ammonium bicarbonate for 45 min at 55 °C. The supernatant was removed, 30 µl of 55 mM iodoacetamide in 50 mM ammonium bicarbonate was added to each gel slice and incubated for 30 min at RT. The gel slices were dehydrated as above. To each dried gel slice, 7–10 µl of 10 ng/µl trypsin gold (Cat.: V5280, Promega, Madison, WI) in 40 mM ammonium bicarbonate/10% acetonitrile were added and allowed to re-swell for ~20 min at 37 °C. The gel slices were overlaid with 20 µl of 40 mM ammonium bicarbonate, 10% acetonitrile and incubated overnight at 37 °C. The peptides were extracted by adding 50 µl of 2% trifluoroacetic acid (TFA) to each gel slice without removing the overlay. The extraction was repeated twice with 33% acetonitrile/1.3% TFA and 63% acetonitrile/0.7% TFA. The extracted peptides were combined and the peptide mixture was dried. The peptide mixture was resuspended in 10 µl of 0.1% TFA and subjected to tandem MS (MS/MS) analysis directly by the mixing 1:2 with 20 mg/ml α-cyano-4-hydroxycinnamic acid matrix solution (LaserBio Labs, Sophia-Antipolis, France) onto a matrix assisted laser desorption ionization (MALDI) target.

Proteomics: Growth and Preparation of Samples

Growth in Fermenters—*L. lactis* NZ9000 pNZ8048 and *L. lactis* NZ9000 pNZcCFTR were grown in 3 L fermenters (Applikon) in M17 medium supplemented with glucose (1%) and chloramphenicol (5 µg/ml). The temperature was set at 30 °C and the pH was maintained at 6.5 during growth by addition of KOH. At an OD₆₀₀ of 0.5 900 ml of the culture was removed and to the remaining culture Nisin A was added (1:5000 dilution of the supernatant of a culture of *L. lactis* NZ9700). After 1 h and 4 h of induction 900 ml of the culture was collected. Cell were spun down (6800 × *g* for 15 min, 4 °C), and pellets were washed once with 10 mM KP_i pH 7.5. The washed cell pellets were frozen in liquid nitrogen and stored at –80 °C.

Isolation of Membrane and Soluble Protein Fractions—The cell pellets were resuspended in 10 mM KP_i pH 7.5 at an OD₆₀₀ of 50. To 6 ml of the suspension MgCl₂ was added (1 mM final concentration) and the cells were disrupted at 39 kPsi with a Constant Systems cell disrupter. The cells were passed through the disrupter cell twice. EDTA was added (15 mM) to the suspensions and they were incubated on ice for 15 min.

To remove nonbroken cells the crude cell lysates were centrifuged for 15 min at 12,000 × *g* at 4 °C. The supernatant was carefully recovered and subsequently centrifuged at 267,000 × *g* for 15 min at 4 °C. The supernatant, containing the soluble protein fraction was carefully pipetted off and stored at –80 °C. Residual supernatant was completely removed from the membranes pellet. The membranes

were washed once with 1 ml 10 mM KP_i containing 10% glycerol. The pellets were finally resuspended in 500 μ l 10 mM KP_i, 10% glycerol and stored at -80°C . Protein concentrations were determined with the BCA kit (Pierce/Thermo Fisher, Waltham, MA).

Sample Preparation for Strong Cation Exchange/ Reverse Phase-Liquid Chromatography (SCX/RP-LC) and iTRAQ Labeling—For trypsinization, 100 μ g of protein (when used for 4-plex iTRAQ labeling, experiment A) or 50 μ g (when used for 8-plex iTRAQ labeling, experiment B) was resuspended in 20 μ l of 500 mM TEAB, 2% acetonitrile plus 0.08% SDS. Reduction of disulfide bonds with Tris(2-carboxyethyl) phosphine hydrochloride, cysteine-modification with methyl-methanethiosulfonate (MMTS) were performed according to the manufacturer's protocol for iTRAQ (Applied Biosystems, Foster City, CA). For enzymatic digestion, trypsin gold (Cat.: V5280, Promega) was reconstituted in 500 mM TEAB and 5 mM calcium chloride, and used in 1:6 (μ g/ μ g) trypsin-to-protein ratio. Digestion was performed over night at 37°C . Undigested material was spun down for 10 min at $14,000 \times g$. The pellets were suspended in TEAB/acetonitrile/SDS solution as before and digested for 5 h at 37°C with 0.8 μ g trypsin per sample. The corresponding samples from two digests were combined, freeze-dried and suspended in 15 μ l 500 mM TEAB. The 8-plex iTRAQ labeling was performed according to the manufacturer's protocol with a few modifications. Each label was reconstituted in 210 μ l 100% isopropanol and to each sample of 15 μ l, 100 μ l reconstituted label was added, so that each label was used for two samples. The four-plex iTRAQ labeling was performed according to the manufacturer's protocol except that each label was resuspended in 200 μ l ethanol and combined with 20 μ l tryptic digest. The samples were incubated for at least 2.5 h at room temperature and stored at -20°C until required. Organic solvent (isopropanol or ethanol) was removed by evaporation. Each sample was suspended in 100 μ l water. From each sample, 50 μ l were combined (200 μ g) and concentrated to a volume of 250 μ l. The same volume of twofold concentrated SCX buffer A (see below) was added, the pH was adjusted to 2.7 with phosphoric acid. The peptide mixture was subjected to chromatography and mass spectrometry analysis.

Refractionation of Peptides on SCX—For off-line peptide pre-fractionation, a silica-based Polysulfoethyl Aspartamide SCX column was used (Cat.: 202SE0502 PolyLC Inc., Columbia USA). The column was run at a flow rate of 200 μ l/min on an AKTA purifier (GE Healthcare). Gradient solutions A: 10 mM triethylammonium phosphate, pH 2.7, 25% acetonitrile; B: 10 mM triethylammonium phosphate, pH 2.7, 25% acetonitrile, 500 mM KCl. Gradient conditions: column equilibration with five column volumes (CV) (1 CV = 0.7 ml) of 100% A. Peptides were loaded in 100% A and the column was washed with 10 CV at 100% A. Peptides were eluted: 1) 0 to 5% B in 5 CV; 2) followed by 12 to 30% B in 10 CV; and 3) 24–60% B in 5 CV. Fractions of elution steps 1 and 2 were collected every 45 s, and fractions of the elution step 3 were collected every 1 min in a 96-well plate. Eluted peptides were dried in a vacuum centrifuge and resuspended in 50 μ l of 0.1% TFA. Depending on the complexity, either separate fractions or pools of two fractions were analyzed by RP-LC MALDI-time-of-flight (TOF)/TOF.

RP-LC and MALDI-TOF/TOF analysis—Peptides were trapped on a pre-column (300 μ m \times 5 mm, C18 PepMap300, LC Packing) and then separated on a C18 capillary column (C18 PepMap 300, 75 μ m \times 150 mm, 3 μ m particle size, LC-Packing) mounted on the Dionex Ultraflex 3000 LC system (LC Packings, Amsterdam, The Netherlands). Mobile phase solutions contained A: 0.05% TFA; B: 0.05% TFA, 80% acetonitrile. Gradient conditions: equilibration of column, binding and washing of peptides was performed with 3% B, elution with 3 to 50% B in 60 min at a flow rate of 300 nL/min. The eluting peptides were mixed 1:4 with 2.2 mg/ml α -cyano-4-hydroxycinnamic acid matrix (LaserBio Labs, Sophia-Antipolis, France) and spotted directly onto a

MALDI target (12 s \times 260 spots), using a Probot system (LC Packings, Amsterdam, The Netherlands). Peptides were analyzed with a 4800 Proteomics analyzer MALDI-TOF/TOF mass spectrometer (Applied Biosystems).

The MALDI-TOF/TOF was operated in reflectron positive ionization mode in the m/z range 900–4000. The 15 most intense peaks above the signal-to-noise threshold of 120 from each MS spectrum of odd-numbered RP-LC runs were selected for MS/MS fragmentation in the m/z range from 900 to 2000. The 10 most intense peaks above the signal-to-noise of 50 were selected from each MS spectrum of even-numbered RP-LC runs in the m/z range from 2000 to 4000. The MS/MS spectra were acquired using 2 kV acceleration voltage and air as collision gas at 5×10^{-7} Torr. The precursor mass transmission window was set to 300 (full width at half maximum, FWHM) for peptides in the m/z range of 900–2000, and to 200 (FWHM) in the range of 2000–4000 m/z . The peak-lists of the acquired MS/MS spectra were generated, using default settings and the S/N threshold of 10. The MS spectra were calibrated in the plate model mode, using 4700 calibration mixture (Applied Biosystems). MS/MS calibration of the instrument was performed when required, using ACTH 18–39 ($m/z = 2465.199$) fragment ions.

Database Search and Criteria for Protein Identification—MS/MS peak-lists were extracted by the ProteinPilot software, version 2.0, using default parameters and were automatically submitted to a database search. All MS/MS spectra were analyzed using Mascot (Matrix Science, London, UK; version 2.0) and X!Tandem (www.thegpm.org; version 2007.01.01.1). Mascot and X!Tandem were set up to search a combined *L. lactis* sp. *cremoris* MG1363 database, allowing one missed cleavage of the digestion by trypsin. The database was created by combining forward and reversed entries of the *L. lactis* proteome (release version 31.08.07) and included sequences of porcine trypsin (NCBI accession: P00761), human keratins (P35908, P35527, P13645, NP_006112), chloramphenicol acetyltransferase (P00485), replication protein A (Q04138), and the human CFTR (NCBI accession: NP_000483) containing in total 4902 protein entries. Mascot and X!Tandem searches were performed with a fragment ion mass tolerance of 0.30 Da and a parent ion tolerance of 200 ppm. MMTS modification of cysteine and Applied Biosystems 4-plex or 8-plexed iTRAQ quantitation chemistry of lysine and the N terminus were specified in Mascot and X!Tandem as fixed modifications. Deamidation of asparagine and glutamine, oxidation of methionine and Applied Biosystems 4-plex or 8-plexed iTRAQ quantitation chemistry of tyrosine were specified in Mascot and X!Tandem as variable modifications.

Scaffold (version Scaffold-2_02_03, Proteome Software Inc., Portland, OR) was used to validate MS/MS based peptide and protein identifications. Peptide identifications were accepted if they could be established at greater than 95.0% probability as specified by the Peptide Prophet algorithm (22). Protein identifications were accepted if they could be established at greater than 99.0% probability and contained at least 2 uniquely identified peptides. Protein probabilities were assigned by the Protein Prophet algorithm (23). Proteins that contained similar peptides and could not be differentiated based on MS/MS analysis alone were grouped to satisfy the principle of parsimony. Those peptides were removed from the dataset when quantification was performed. The false positive rate was calculated by dividing 2 times the number of proteins identified in the reversed database by 4902, the sum of all proteins identified in forward and reversed versions of the database. In all measured samples, no hits from the reversed database were detected, using the criteria described above.

Relative Quantification of Protein Expression—The relative quantification was based on peptides that were chemically labeled with isobaric reagents, using the 4-plex or 8-plex iTRAQ technique. The

quantification information was obtained from the peak areas of the reporter ions (m/z 112.2, 113.2, 114.2, 115.2, 116.2, 117.2, 118.2, 119.2, and 121.2). The peak areas were extracted from the MS/MS spectra by the ProteinPilot software using default settings as specified by the ProteinPilot for the 4800 MALDI instruments (Applied Biosystems). The peak areas were corrected for isotopic impurities by the ProteinPilot using the information provided by the manufacturer in the Certificate of Analysis for each iTRAQ batch. To select quantification data, those ratios were removed where the peak area of one reporter ion was below the signal-to-noise threshold of 10.

The global bias correction was performed for all identified peptides. The bias correction factor for a given iTRAQ ratio (e.g. 113/114) was calculated as the sum of all reporter peak areas in all measured spectra from one iTRAQ reagent (e.g. 114) divided by the sum of reporter peak areas of another reagent (e.g. 113). To obtain the bias-corrected peptide iTRAQ ratios, all measured ratios (in this example all 113/114 ratios) were multiplied by the correction factor. The bias-corrected peptide ratios of the same protein were weight-averaged and protein iTRAQ ratios were obtained according to the method used by the ProteinPilot software (Applied Biosystems). Peptides that matched to multiple proteins were excluded from quantification.

The relevant protein and peptide data and given in supplemental Tables S5 and S6.

Statistical Analysis

Identifying Significantly Changed Protein Abundances—To identify proteins with significantly changed abundances two different methods were used depending on the number of available replicate values. Rank Sum analysis was used for the comparison of the CFTR expressing strain *versus* the control strain at the 4 h time point, where four independent replicates were available. Rank Sum is a nonparametric statistical method based on the Rank Product analysis (24, 25), which allows the data from biological replicates to be analyzed in a robust way. For the Rank Sum analysis the weighted protein ratios for each of the four replicate samples were calculated as described above and sorted in descending order. Ranks were assigned to each protein, so that the protein with the highest ratio had rank 1, and the protein with the lowest ratio had a rank corresponding to the total number of identified proteins. To combine the protein ranks of all four measured replicates, the sum of ranks across replicates was calculated, sorted in descending order and ranked again. The p value for each protein was calculated by comparing its rank sum with the result of 1000 permutations of the list using the RankProd package for R (26). The resulting p values were then corrected for multiple testing using the adaptive false discovery rate (FDR) control method (27), giving the so-called q -values. This was done using the *fdrtool* R package (28). An FDR rate of 10% was used as the threshold for selecting proteins with significantly changed expression. The lists of proteins sorted by the RankSum were used as input for iterative Group Analysis (29) as described before (30) to analyze the ribosomal proteins.

For all the other comparisons (0 h–1 h; 0 h–4 h; 1 h–4 h for both the CFTR expressing or control strain; 0 h–0 h and 1 h–1 h CFTR expressing *versus* control strain) only two biological replicates were available, and therefore a different analysis was done. For each of these comparisons the iTRAQ log ratios from the two biological replicates were averaged and the distribution of the values was compared with the distribution of the iTRAQ ratios obtained from the comparison between the two biological controls that should be identical (Control strain 1 h after induction from two different replicate fermentations, supplemental Fig. S2). As described in the results section the threshold for selecting proteins with significantly changed expression was chosen based on this comparison.

RESULTS

CFTR Expression by *L. lactis*—The *cftr* gene was fused to the coding sequence for an N-terminal (nHis-CFTR) or C-terminal (CFTR-cHis) His-tag, or both (nHis-CFTR-cHis) and was cloned in plasmid pNZ8048 for expression in *L. lactis*. Expression of genes from this plasmid is under control of the Nisin A inducible promoter. The *cftr* containing plasmids were transformed to *L. lactis* expression strain NZ9000. No mutations or gene rearrangements were observed in the expression plasmid, even after many generations of growth of the transformed strains, indicating that the gene was stable and well tolerated by *L. lactis*, in contrast to what has been reported for *E. coli* (31, 32).

L. lactis strains with the plasmids for nHis-CFTR, CFTR-cHis or nHis-CFTR-cHis were cultivated and *cftr* expression was induced with Nisin A in the exponential growth phase (OD_{600} of 0.5). Induction of the expression with Nisin A severely affected growth, and at the time of harvest (2 hours after induction) the cultures of the *cftr* expression strains had reached much lower cell densities than control cultures (supplemental Fig. S1). Cells were lysed, membranes were isolated, and the proteins in the membrane fraction were separated by SDS-PAGE. CFTR expression was examined by Western blot analysis, using two different monoclonal antibodies, which recognized the engineered His-tags or the native C terminus of the CFTR protein. The nHis-CFTR protein could be detected by both antibodies as a band that migrated at an apparent molecular mass of 130 kDa, showing that both the N terminus (His-tag) and the C terminus (epitope of the CFTR specific antibodies) were present, and thus full-length protein had been produced (Fig. 1A and 1B). For detection of CFTR constructs with C-terminal His-tags (CFTR-cHis and nHis-CFTR-cHis), only the anti-His-tag antibodies could be used, because the His-tag on the C terminus prevented detection of the protein by the CFTR specific antibodies. Full-length CFTR-cHis was not detected, but nHis-CFTR-cHis was detected and migrated at approximately the same apparent molecular weight as nHis-CFTR on SDS-PAGE, which again confirmed that the full-length CFTR had been produced by *L. lactis*. In addition to the full-length proteins, a number of smaller fragments were detected which are likely to be degradation products (Fig. 1).

Apparently, the presence of an N-terminal His-tag was necessary for production/detection of full-length CFTR. To investigate further how N-terminal modification affected the production of full-length CFTR, a construct was made with an MBP domain plus a His-tag fused at the N terminus (His-MBP-CFTR). His-MBP-CFTR was detected in *L. lactis* membranes with the anti-CFTR antibodies and had an apparent molecular weight of 170 kDa (Fig. 1A), as expected for the full-length protein. To confirm that the full-length protein was produced, and to obtain an estimate of the expression levels, His-MBP-CFTR was partially purified. Membranes containing

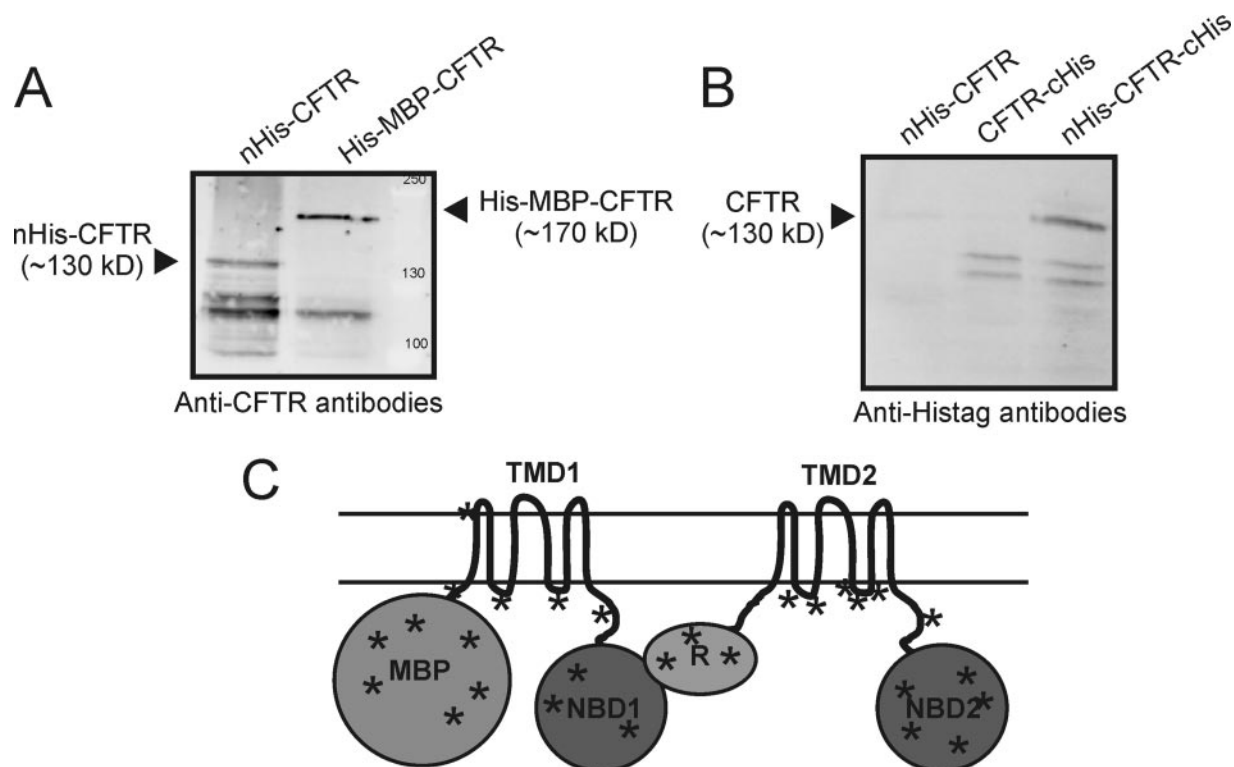


FIG. 1. Expression of human CFTR in *L. lactis*. *A*, Membranes of *L. lactis* expressing His-MBP-CFTR and nHis-CFTR were analyzed by SDS-PAGE/Western blotting. CFTR was detected using anti-CFTR antibodies (clone 24–1, R&D systems). Ten micrograms protein was loaded per lane. *B*, Membranes of *L. lactis* expressing nHis-CFTR, CFTRcHis and nHis-CFTR-cHis were analyzed as described above, but now using anti-His-tag antibodies. *C*, Topology model of His-MBP-CFTR indicating the different domains, and showing positions of the tryptic peptides identified with LC-MS/MS. Peptides derived from all soluble domains of His-MBP-CFTR were found. For a complete list see supplemental Table S2.

His-MBP-CFTR were solubilized with the detergent DDM and subjected to Ni-Sepharose chromatography. On a Coomassie-stained gel a very faint band corresponding to a protein with an apparent mass of 170 kDa was visible in the elution fraction (not shown). Based on the intensity of the Coomassie stained band we estimated that His-MBP-CFTR represented <0.1% of the proteins in the membrane fraction. The stained 170 kDa protein band was excised from the gel, peptides were generated by trypsin hydrolysis, and the peptides were analyzed by MALDI tandem mass spectrometry. Forty-four peptides were identified covering 28% of the protein sequence and including peptides from both the N-terminal domain (MBP) and the most C-terminally located domain (NBD2), again confirming that *L. lactis* had produced the full His-MBP-CFTR fusion (Fig. 1C, and supplemental Table S2).

Consequences of CFTR Overexpression—The above experiments show that full-length human CFTR was produced in *L. lactis* membranes. Although this result is extremely encouraging, the expression levels were too low for functional or structural characterization; in addition expression of CFTR severely affected the growth of *L. lactis* (supplemental Fig. S1). To investigate the effect of CFTR expression on the physiology of *L. lactis*, and to identify why *L. lactis* produced

only small amounts of CFTR, a proteomic approach was followed using quantitative mass spectrometry. The experimental setup is outlined in Fig. 2. Two replicate fermentations (Replicate 1 and 2 in Fig. 2) were carried out both of *L. lactis* containing the expression plasmid for nHis-CFTR-cHis, and of *L. lactis* containing the empty plasmid pNZ8048. All cultures were grown in fermenters of 3 liter volume, with temperature (30 °C) and pH control (6.5). The inducer Nisin A was added to both the control and the expression strains in the mid-exponential growth phase ($OD_{600} \sim 0.5$, supplemental Fig. S1). 900 ml of cells was harvested at each of three timepoints: just before the addition of Nisin A (time point 0 h), and at 1 h and 4 h after induction, yielding a total of 12 cell-samples (3 timepoints per fermentation) (Fig. 2 and supplemental Fig. S1).

Each of the 12 cell-samples was lysed, and membrane and soluble fractions were isolated (abbreviated as M and S, respectively in Fig. 2), resulting in 24 protein samples. The separation of membrane and soluble fractions was done to facilitate the identification of low-abundance membrane proteins, and to follow the possible redistribution of proteins between the membrane soluble fractions upon overexpression (see *Discussion*). The membrane and soluble fractions were kept separate during the subsequent analysis.

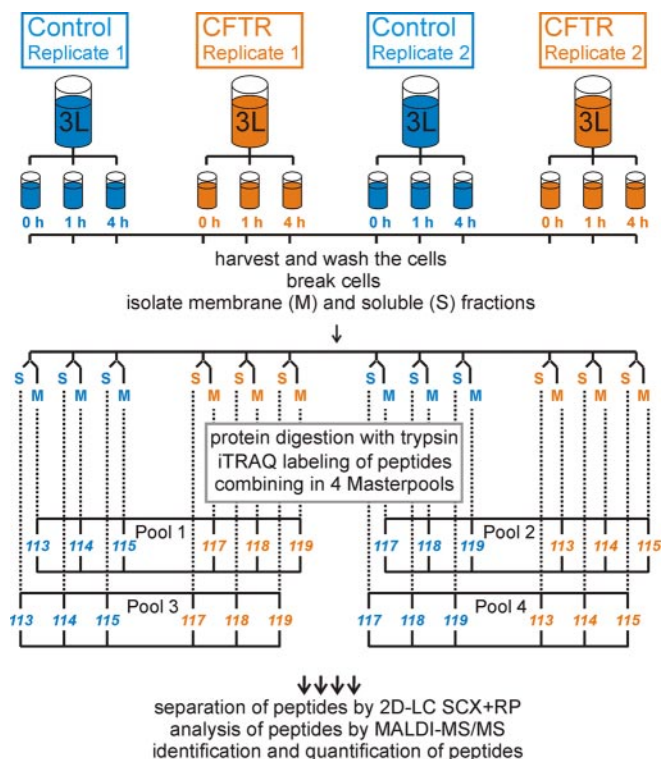


FIG. 2. Workflow of the proteomics study. To compare relative protein abundance in the control and CFTR-expression strains, the cells were grown in fermenters under controlled conditions. Each strain was grown twice (biological replicates). To follow the relative changes in expression in the CFTR and the control strain in time, three cell aliquots (900 ml each) were harvested immediately before induction of CFTR-expression, and 1 h and 4 h after induction, resulting in 12 cell samples. The cells were lysed and the cell lysate was fractionated into the membrane (M) and soluble (S) fractions by differential centrifugation. Thus 24 protein samples were obtained from four cultures. Each protein sample was digested with trypsin to create peptide samples and the peptides were labeled with the isobaric iTRAQ reagents. Eight different iTRAQ reagents were used, termed 113, 114, 115, 116, 117, 118, 119, 121 (for the mass of the reporter fragment). Six peptide samples labeled with different reagents (three from the control strain, and three from the CFTR-expression strain) were combined in one “Master pool” (for details see supplemental Fig. S2). The 24 labeled peptide samples were combined in four Master pools. Each Master pool of labeled peptides was subjected to two-dimensional chromatography separation, using off-line Strong Cation Exchanger in combination with the Reversed-phase Chromatography. Separated peptides were collected on a MALDI-target and analyzed by tandem MS/MS. The obtained MS/MS spectra were analyzed by Mascot and ProteinPilot software which provided identification and quantification information for each spectrum. The identified and quantified peptides derived from the same protein were integrated, resulting in identification and quantification information of proteins.

The 24 protein samples were digested with trypsin, yielding 24 peptide-samples, which were divided into four sets, each containing six different peptide-samples (Fig. 2). Three of these peptide-samples were derived from control cells (corresponding to the three timepoints 0 h, 1 h and 4 h of the same fermentation), and the other three from the CFTR ex-

pression cells. This was done separately for the membrane and the soluble fractions, and separately for the replicate fermentations.

Each peptide-sample in the set of six was labeled with a different isotope label, for which isobaric iTRAQ reagents from the 8-plex iTRAQ kit were used, and the six differentially labeled samples were combined into a “Master pool.” The Master-pool was supplemented with two more peptide-samples (labeled with yet two different iTRAQ labels from the 8-plex iTRAQ kit): (1) a “technical control,” which was a peptide sample identical to one of the six peptide-samples already present, but labeled with a different isotope label; (2) a “biological control,” which was related to one of the six peptide-samples already present but obtained from the replicate fermentation. The iTRAQ labeling scheme is shown in supplemental Fig. S2. Different label combinations (label swaps) were used in the different Master pools.

The labeled peptide mixtures in the four Master pools were fractionated using cation exchange and reversed phase chromatography, and the eluting peptides were analyzed by MALDI-MS/MS, which provided both identification and quantification data. The fragmentation spectrum was used to identify each peptide, and the areas of the eight different reporter peaks from the iTRAQ labels were measured for later comparative quantification. The identification and quantification data of different peptides originating from the same protein were integrated, and the resulting protein data from the different replicates were combined, yielding two lists of proteins (744 from the membrane fractions and 688 from the soluble fractions) that were fully quantified using iTRAQ in both replicates (supplemental Tables S3 and S4).

The experimental design allowed for the comparison of the relative protein abundances (ratios of the quantified iTRAQ reporter peaks) for each pair of samples present in the Master-pool. Because there were eight peptide samples in the Master pool, a total of 28 different iTRAQ pairs (ratios) could be calculated ($8!/2!(8-2)!$) for each protein. Only nine of these ratios were biologically relevant: (a) the changes in protein levels during the time course of the expression (0 h versus 1 h; 1 h versus 4 h; 0 h versus 4 h) for both the control strain and the CFTR expression strain (six iTRAQ ratios in total; Fig. 3, dashed lines); and (b) the differences in protein levels between the control strain and the CFTR expression strain at each of the three time-points (0 h, 1 h, 4 h; three iTRAQ ratios; Fig. 3, solid lines). The technical and biological controls which had been taken along in each 8-plex iTRAQ experiment resulted in two more relevant ratios for control purposes (supplemental Fig. S2).

In supplemental Tables S3 and S4, the averaged iTRAQ ratios from the two biological replicate (expressed as logarithms, \log_{10} -ratios) for each of the nine biologically relevant comparisons are given for all of the identified proteins. Also the averaged iTRAQ ratios for the two biological controls samples and the technical controls are listed.

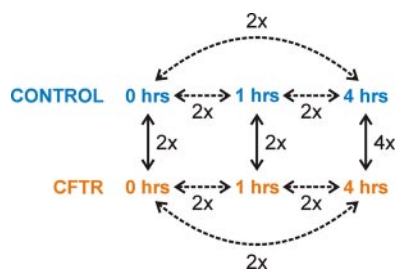


FIG. 3. Schematic representation of a Master pool and an outline of the meaningful comparisons of the relative protein abundances. Each Master pool contained peptide samples representing three time points of the control strain and three time points of the CFTR-expression strain (0 h, 1 h, 4 h after induction expression). The expression levels of proteins could be followed as function of the time *within* the control and CFTR-expression strains (dashed lines). Furthermore, the relative changes in protein abundance could also be calculated *between* the control and the CFTR-expression strains at three of the time points (solid lines). All the comparisons were based on two independent biological replicates (Fig. 2), indicated by 2 \times . However, the comparison between the CFTR expressing strain and the control strain at the 4 h time point was repeated two more times in order to obtain four replicate values (4 \times).

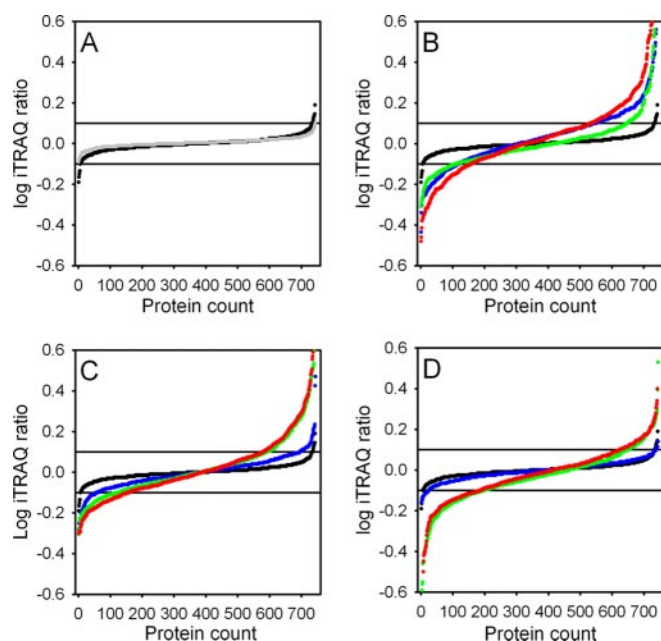


FIG. 4. Distribution of iTRAQ log ratios of the 744 proteins identified in the membrane fractions in the various comparisons (cf Fig. 3). The averaged values of two biological replicates are shown. Horizontal reference lines are drawn at the cutoff values of -0.1 and 0.1 . A, Technical (Gray) and biological controls (Black). B, Biological controls (Black), comparisons 1 h–0 h (Blue), 4 h–1 h (Green) and 4 h–0 h (red) for the control cells. C, Biological controls (Black), comparisons 1 h–0 h (Blue), 4 h–1 h (Green) and 4 h–0 h (red) for the CFTR expressing cells. D, Biological controls (Black), comparisons CFTR expressing cells *versus* control cells at timepoints 0 h (Blue), 1 h (Green), and 4 h (red).

Control Experiments: Technical and Biological Replicates—To determine which proteins had changed in abundance, the distributions of iTRAQ log ratios in the nine

biologically relevant comparisons (Fig. 3 and supplemental Tables S3 and S4) were evaluated against the distribution in the biological control (Fig. 4). The biological control consisted of two samples from the *same* condition (1 h of induction; control cells) but from two *different* fermentations (supplemental Fig. 2, indicated with asterisk) and thus should be identical. Ninety-eight percent of the iTRAQ log-ratios of the biological control fell in the window between -0.1 and 0.1 (Fig. 4A). The distribution of the iTRAQ log-ratios of the biological control was similar to the distribution of the technical control (gray line in Fig. 4A) showing that the biological noise was low. In contrast, the distribution of the iTRAQ log ratios was different when the protein abundances in the samples taken after 1 h and 4 h of induction were compared with the time point 0 h, both in the control and the CFTR-expressing cells, and both in the membrane and soluble fractions (Fig. 4B and 4C for the membrane fraction). The distribution of iTRAQ ratios was also different from the biological control when the protein abundances were compared *between* CFTR expressing cells and control cells at the timepoints 1 h and 4 h (Fig. 4D). For example, at the 4 h time point (column M in supplemental Tables S3 and S4) $\sim 40\%$ of the iTRAQ log ratios were higher than 0.1 or lower than -0.1 (red dots in Fig. 4D). In Fig. 5 and supplemental Tables S3 and S4, numbers in green and red indicate iTRAQ log ratios above 0.1 and below -0.1 respectively. These thresholds were used to analyze trends in the data as described below.

Time Series: Patterns—We identified several patterns of change as a function of induction time when the samples taken after 1 h and 4 h of induction were compared with the time point 0 h, both in the control and the CFTR-expressing cells, and both in the membrane and soluble fractions (supplemental Tables S3 and S4). When the expression level of a protein increased or decreased in time, the increment or decline could follow several patterns: (1) “gradual,” *i.e.* it increased or decreased after 1 h of expression when compared with the zero time point, and increased or decreased even more after 4 h of expression (*e.g.* FruC and FruD, Fig. 5A); (2) “leveling off,” *i.e.* the change within 1 h was followed by constant levels upon further expression (*e.g.* the Pur proteins in the control cells, Fig. 5A); (3) “delayed,” *i.e.* no changes after 1 h followed by a change after 4 h (*e.g.* the Pur proteins in the CFTR expressing cells or the subunits of the pyruvate dehydrogenase complex in both the control and expression strains, Fig. 5A); (4) “opposite,” *i.e.* a change in expression after 1 h is followed by an opposite change after 4 h (*e.g.* RibA in Fig. 5A).

Importantly, the patterns of change in time for different subunits of known complexes, or for different proteins coded by the same operon, were very similar, indicating a high level of consistency in the results. For instance, the four subunits of the pyruvate dehydrogenase complex mentioned above (Pdh proteins), all showed the “delayed” pattern of change (Fig. 5A). Similarly, the subunits of the Opp system, an ABC trans-

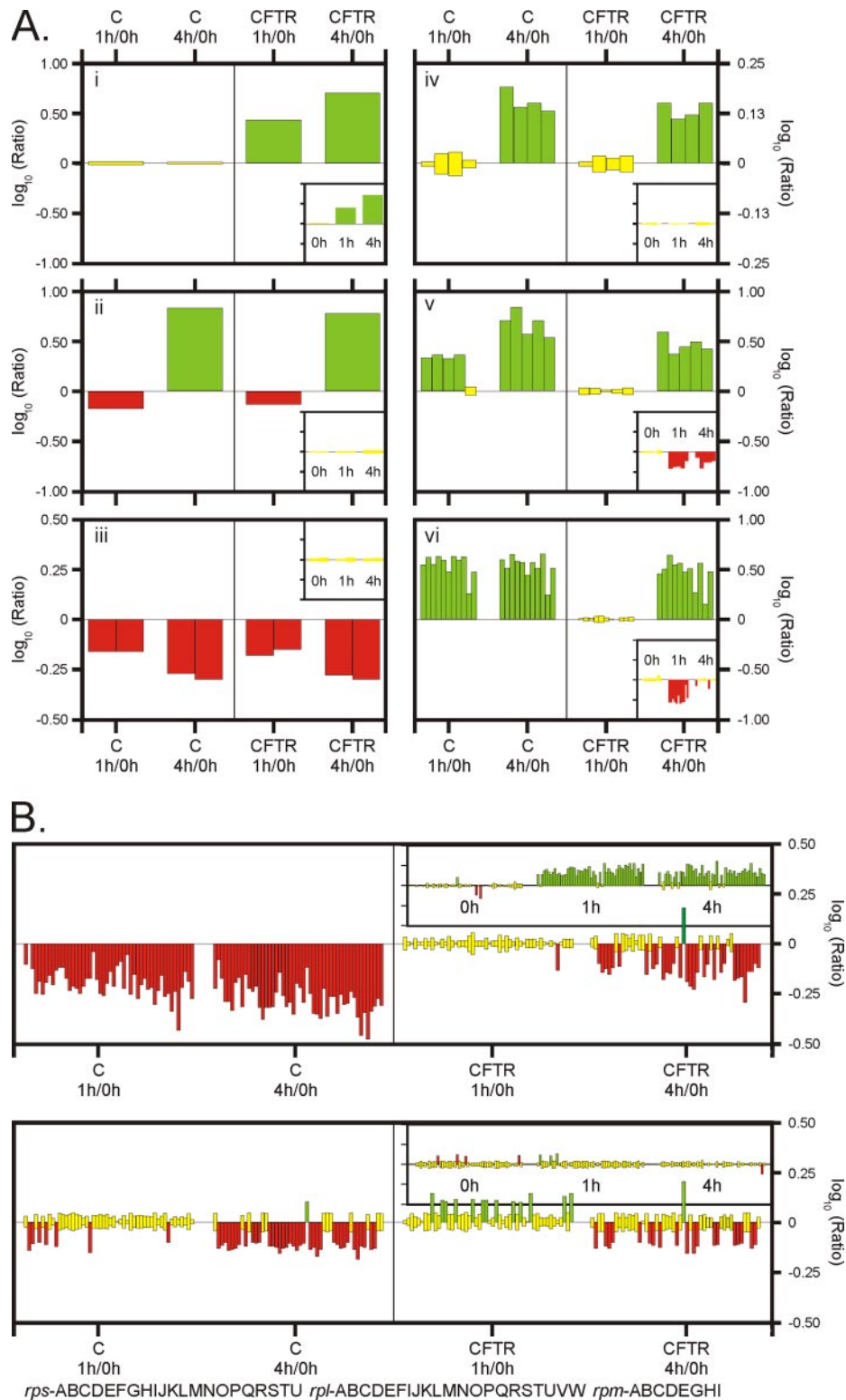


FIG. 5. **Examples of proteins changing abundance upon induction.** Each bar in the panels and insets represents one protein. The height of the bar indicates relative difference in abundance of protein (logarithm of the iTRAQ ratio). On the left-hand side of each panel, the relative changes in protein expression *within* the control strain upon induction are presented (comparing 0 h and 1 h, and 0 h and 4 h). On the right-hand side of each panel, the relative changes in protein expression in the CFTR-expression strain are presented. The apparent changes in protein abundance *between* the CFTR- and the control strain (at time point 0 h, 1 h, and 4 h) are shown in the insets. Color: red, green and yellow colors indicate significantly decreased, increased and unchanged protein abundance, respectively. A, Panel i: CFTR; Panel ii: RibA (riboflavin

porter for peptides, showed the same pattern of expression (“gradual” or “delayed” in the control and expression strains, respectively, Fig. 5A). In addition, PepO, which is coded by the same operon as the *opp* genes, also displayed the same pattern of changes. Another example of proteins coded by an operon are the Pur proteins, all of which showed the same pattern of change (“leveling off” and “delayed” in the control cells and expression cells, respectively, Fig. 5A).

Control versus CFTR-expressing Cells—The relative protein abundances *between* control cells and CFTR expressing cells at the timepoints 1 h and 4 h after induction were also compared. Differences resulted from unequal patterns of time-dependent changes in protein levels between the control and the CFTR-expression cells. At each time point thirteen different combinations of changes in proteins levels in the control and expression cells are possible (Fig. 6). If no differences are observed for the abundance of a protein at a time point, this could be the result of the absence of time-dependent changes in both the control and CFTR-expressing cultures (Fig. 6, middle row, pattern #1), but it also could result from similar extents of up- or down-regulation of in both strains (Fig. 6, middle row, patterns #2 and 3, respectively). An example of pattern #2 is the pyruvate dehydrogenase complex where all subunits were up-regulated to a similar extent in both the control- and the expression-strain, resulting in an apparently unchanged expression when comparing the two strains with each other.

An apparent elevation of a protein level as a consequence of CFTR-overexpression could be the result of up-regulation in the CFTR-strain and concomitantly either no changes (Fig. 6, bottom row, pattern #1), down-regulation (Fig. 6, #2), or up-regulation to a lesser extent (Fig. 6, #3) in the control strain. An apparent up-regulation also could be a result of down-regulation in the control strain and either no changes in the CFTR expression strain (Fig. 6, #5) or a weaker down-regulation (Fig. 6, #4). An example of pattern #1 is, of course, the CFTR protein itself: its abundance “gradually” increased in time in the CFTR-expressing strain, whereas the protein was absent in the control stain (Fig. 5A). In theory, the iTRAQ ratio, when comparing CFTR abundance in the expression strain and in the control strain, should be infinite (division by zero). However, this was not the case because iTRAQ quantification tends to dampen to ratio of proteins that are of very low abundance in one of the two strains (33). Nonetheless, the CFTR protein had one of the highest iTRAQ ratios found.

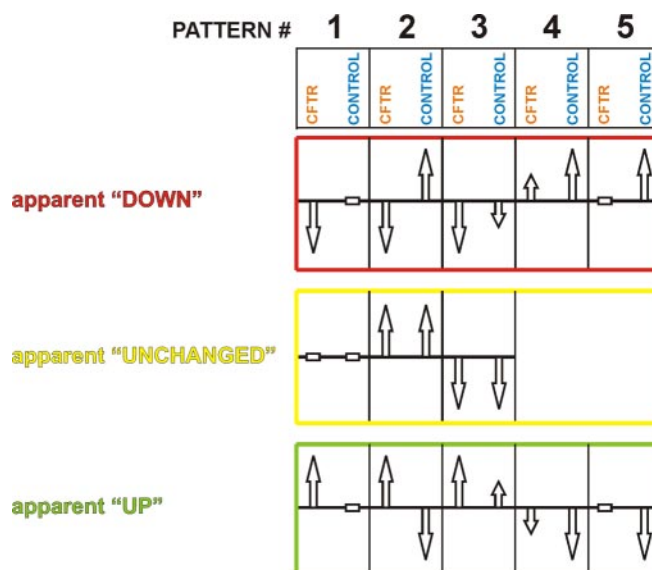


Fig. 6. Patterns of relative changes. At any given time point, the abundance of a protein in the CFTR expression strain can be the same (yellow), increased (green) or decreased (red) compared with the control strain. These *apparent* effects depend on the changes in abundance of the proteins as function of the time within the control and CFTR-expression strains. Arrows pointing upward and downward indicate that protein abundance respectively increased or decreased in time. A horizontal bar indicated unchanged levels in time. An apparently unchanged expression level in the CFTR/control comparison is the result of *equal* changes in the control and CFTR-expression strains, respectively (*middle* panel). An apparent down-regulation in the CFTR/control comparison at a time point (*upper* panel) can be caused by decreased protein levels in the CFTR-expression strain and either unchanged levels in the control strain (*upper* panel, pattern #1), increased levels in the control strain (*upper* panel, pattern #2), or decreased levels in the control strain but of a lower magnitude than in the CFTR-strain (*upper* panel, pattern #3). Furthermore, an apparent down-regulation can be the consequence of increased protein expression levels in the control-strain, combined with either unchanged levels in the CFTR-strain (*upper* panel, pattern #5), or increased levels in the CFTR strain of a lower magnitude than in the control strain (*upper* panel, pattern #4). An apparent increase in protein abundance between the CFTR- and control strains (*bottom* panel) is caused by the opposite effects as an apparent decrease.

Apparent down-regulation at the 1 h and 4 h time-points also could be the results of several scenarios (Fig. 6, upper row). For instance, the proteins of the oligopeptide transport system Opp followed pattern #4: in the control strain the abundances of all subunits were increased after 1 h of expression and further increased after 4 h (“gradual”, Fig. 5A). In contrast, the same proteins had not changed in abundance in

biosynthesis protein); Panel iii: Proteins encoded by the fructose operon: FruC (fructose 1-phosphate kinase) and FruR (transcriptional regulator of the fructose operon). Panel iv: Proteins encoded by the pyruvate dehydrogenase operon: PdhA, PdhB and PdhC are the subunits of the pyruvate dehydrogenase complex; PdhD is dihydrolipoamide dehydrogenase. Panel v: Proteins encoded by of the oligopeptide transport system operon: OppA, OppB, OppD and OppF are subunits of the oligopeptide ABC-transporter (OppC was not identified); PepO is the endopeptidase O. Panel vi: Proteins encode by the purin operon. PurC, D, E, F, H, K, L, M, Q, R, S. *B*. Apparent changes in abundance of ribosomal proteins in the membrane and soluble fractions. Top panel: membrane fraction, bottom panel: soluble fraction. The following ribosomal subunits are shown: rpsABCDEFGHIJKLMNQRSTU, rplABCDEFGHIJKLMNQRSTU, rpmABCDEFGHI.

the CFTR strain after 1 h, but did increase in abundance after 4 h (“delayed”). So, even though the levels of the Opp proteins increased in time in the CFTR expression strain, they increased at a lower rate than in the control strain, resulting in an apparent decrease of protein abundances when comparing the two strains at any given time point. Another example for the apparent lowering of protein levels as the consequence of CFTR-overexpression was seen for the proteins of the purine metabolism. PurB, PurC, PurD, PurH, PurK, and PurL, were up-regulated in the control cells when comparing time point 1 h with time point 0 h, but remained constant when comparing timepoints 4 h with time point 1 h (“leveling off,” Fig. 5A). In contrast, in the CFTR-expressing cells the protein levels remained constant or slightly increased during the first hour of induction, and further increased during the next 3 h to levels comparable to the control cells (“gradual” or “delayed,” Fig. 5A). Therefore, when comparing the CFTR-expression strain to the control, the relative abundances of these proteins were apparently decreased at 1 h (Fig. 6, upper row, pattern #4 or #5), but were unchanged after 4 h (Fig. 6, middle row, pattern #2).

The data described above, which showed consistent time-dependent changes in protein abundances for the various comparisons, were based on two biological replicates only. Therefore, to improve the confidence of the analyses and to be able to apply more rigorous statistical criteria to find significantly up- or down-regulated proteins we repeated the comparison between CFTR expressing cells *versus* control cells at the time point 4 h two more times, so as to get four replicates (Fig. 4 and supplemental Fig. S2). Time point 4 h was chosen for the extra replicates, because we had noticed that the relative abundances of almost all proteins (CFTR expression strain *versus* the control strain) were qualitatively similar at timepoints 1 h or 4 h after induction (down- or up-regulation or no change), but the extent of change (absolute values of the iTRAQ ratios) were generally larger, and thus more reliable, at the 4 h time point. The extra replicates values were obtained essentially in the same way as described in Fig. 2, but in this case the 4plex iTRAQ reagents were used. For the iTRAQ labeling scheme see supplemental Fig. S2 and for the values see supplemental Tables S3, S4 and S5. Seven hundred and nine and 644 proteins were identified and quantified in the membrane and soluble fractions in all four replicates of the 4 h time point. To find proteins with significantly different abundances the RankSum and FDR algorithms were used as described in the methods section. At the 4 h time point, 147 proteins had significantly changed in abundance in the membrane fraction (70 up and 77 down) and 202 proteins in the soluble fraction (104 up and 98 down) (FDR-corrected *p* values <0.1; supplemental Tables S3 and S4).

Only the proteins that were found to be significantly changed in abundance at the 4 h time point using the RankSum/FDR criterion have been included in the discussion on the physiology below. The observed time-dependent changes

in the protein abundances based on two biological replicates (Figs. 3, 4, and 5 and supplemental Tables S3 and S4) have been used in the discussion only for those proteins that had significantly changed in abundance according to the stringent analysis based on four replicates.

DISCUSSION

Production of sufficient amounts of well-folded membrane protein is a major bottleneck in membrane protein research. CFTR is no exception, and biochemical/biophysical studies on the protein are hampered by low yields of correctly folded and stable protein. Here we have used the prokaryotic expression host *L. lactis* to express full-length human CFTR. To the best of our knowledge this is the first report of bacterial expression of full-length human CFTR. Although the results are encouraging, the yields of CFTR were too low (<0.1% of membrane protein) for functional/structural characterization. In addition, growth of the cells was severely compromised when expression of CFTR was induced, resulting in low biomass yield and indicating toxicity to the cell. Low yields and growth arrest have been observed upon expression of numerous human membrane proteins in *L. lactis*, also for proteins that could be assayed for function. For instance the human KDEL receptor was shown to be functional in the membrane of *L. lactis* by a ligand binding assay, despite low levels of expression and growth arrest (5). The ligand binding assay for the low-abundant KDEL receptor was possible because a high-affinity radiolabeled ligand was available. Such ligands are not available for CFTR.

In an attempt to understand why the CFTR yields were low, and possibly to remedy the expression bottlenecks, we used quantitative proteomics to characterize the response of *L. lactis* to expressing CFTR in its plasma membrane. In the combined membrane and soluble fractions we identified and quantified a total of 846 proteins, representing 35% of the predicted *L. lactis* proteome. Among the identified proteins were 163 integral membrane proteins, which were strongly enriched in the isolated membrane fractions. The large number of identified proteins allows reliable analysis of the physiological responses of *L. lactis* to the expression of CFTR. The major responses are summarized in Fig. 7, and will be discussed below. To our knowledge this is the first study in which the stress response of *L. lactis* upon membrane protein production is systematically analyzed.

Stress from Protein Misfolding—For the majority of the proteins that had higher abundance in the CFTR-expression strain than in the control strain at the 4 h time point (supplemental Table S3 and S4), the abundance had increased as a function of time in the expression strain, but remained unchanged in the control strain (Fig. 6, bottom row, pattern #1). Almost all of the proteins following this pattern were found to be stress related. A striking example is PacL, a putative cation transporting P-type ATPase (34). When comparing the expression and control strains at the 4 h time point,

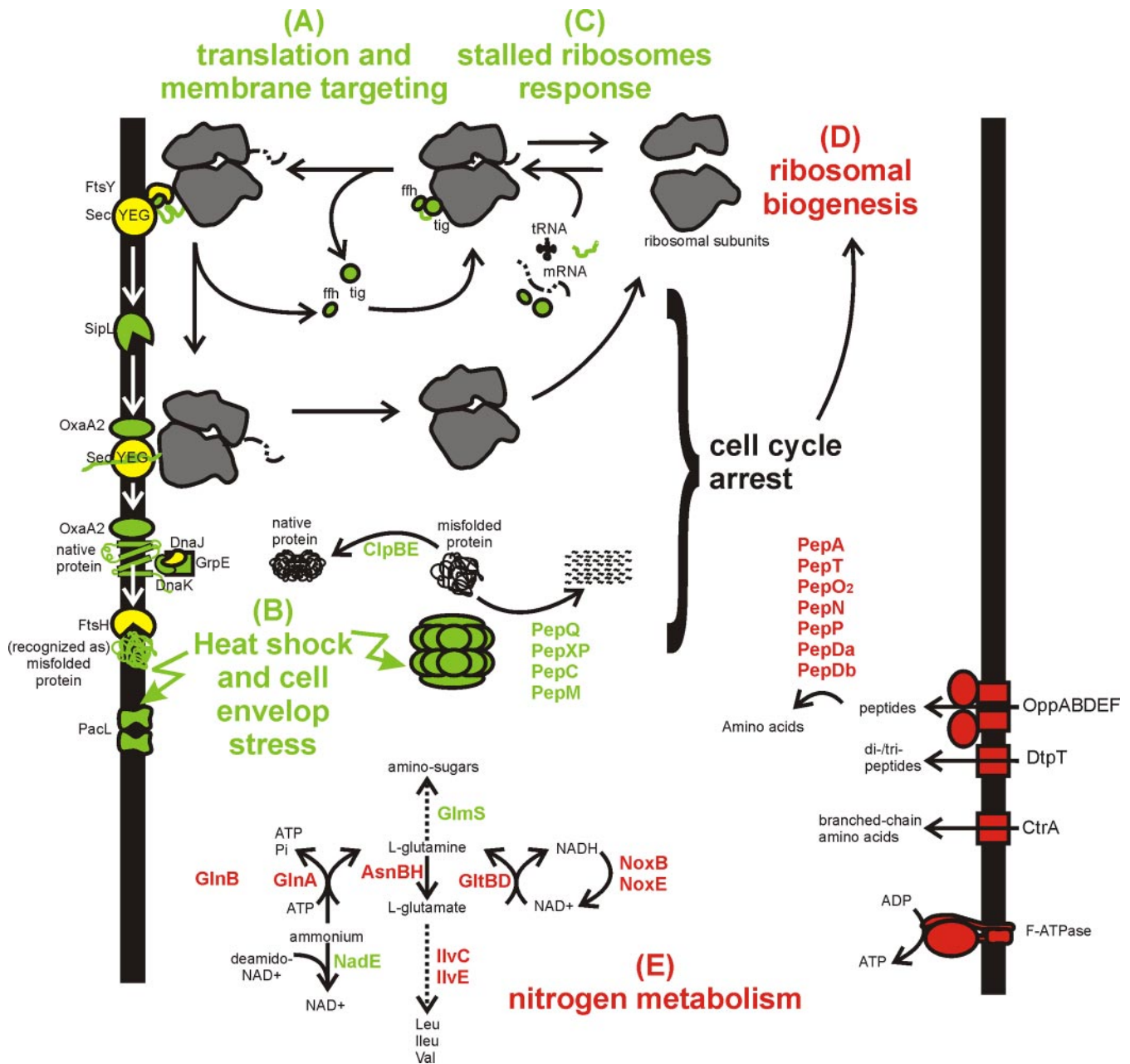


FIG. 7. The physiological responses of the bacterium *Lactococcus lactis* to the production of the human CFTR. Red and green colors indicate proteins that are lower and higher in abundance respectively in the CFTR expressing strain compared with the control strain at time point 4 h after induction. Yellow proteins have the same abundance. A, Nascent chains of membrane proteins emerging from the ribosome are recognized by trigger factor (*tig*) and the signal recognition particle (containing the *ffh* protein) and the complex is targeted to the membrane via the receptor FtsY. The nascent chain is co-translationally inserted into the membrane upon docking on the SecYEG translocon. B, The proper folding of the protein is assisted by membrane-integral (OxaA) and/or cytosolic (DnaJK) chaperones. Misfolded proteins trigger heat-shock and cell envelope stress responses. C, Upon production of CFTR, the stalled ribosomes response is triggered. Also proteins involved in general and oxidative stress responses are up-regulated in response to CFTR production (not shown). D, CFTR production leads to growth arrest which correlates with the reduced ribosomal biogenesis. E, Proteins that become de-repressed in response to limited nitrogen were collectively lower in abundance in the CFTR expressing strain than in the control strain (Opp, DtpT, CtrA, Pep proteases, IlvC, IlvE, GlnA, GlnB, and GltBD). The reduced abundance was caused by a strong up-regulation of these proteins in the control strain.

PacL displayed the highest level of up-regulation (highest iTRAQ ratio) of all identified proteins (supplemental Table S3 and S4). The biological role of PacL is not known, but expression of the protein is under control of the CesSR

two-component system, which orchestrates the response of *L. lactis* to cell envelope stress caused by, for instance, anti-bacterial peptides (35, 36). CesSR regulates the expression of numerous proteins, many of which were also affected in the

CFTR expression strain: the membrane protein chaperone/insertase OxaA2 (YidC homologue), the peptidyl-prolyl isomerase PpiB, CesR itself, and a number of proteins of unknown function were all up-regulated, indicating cell envelope stress.

A second group of stress related proteins that was collectively up-regulated comprised proteins of the heat shock response (37). The chaperones DnaK, GrpE, GroEL, and GroES were all up-regulated in the CFTR expression strain, indicating a response to misfolded proteins. Similarly, ClpB and ClpE, involved in the degradation of misfolded proteins (38), were up-regulated but, surprisingly, DnaJ was not, and its expression pattern was very different from the other heat-shock related proteins. In contrast to the heat shock proteins, the cold shock protein CspE decreased in abundance in the CFTR expression cells.

Other proteins that have been associated with stress responses also increased in abundance upon CFTR expression, including the major stress regulator SpxA, NAD synthase NadE, and endo-1,4- β -xylanase D XynD (involved in cell wall stress). In addition, a number of universal stress proteins, hydrolases and peptidases (PepQ, PepXP, PepC, and PepM) were up-regulated, indicating that these proteins may also be stress-related.

Two proteins that have been reported to be involved in the oxidative stress response (thioredoxin TrxH and thioredoxin reductase TrxB1 (39, 40)) were also up-regulated in the CFTR-expressing strain, whereas their expression levels were nearly unchanged in the control sample. In contrast, many other proteins involved in the oxidative stress response were very differently regulated. In control cells numerous proteins involved in the response to oxidative stress were up-regulated at the 1 h and 4 h time-points, including SodA (superoxide dismutase), NoxB (NADH dehydrogenase), NoxE (NADH oxidase), Rex (redox sensing transcriptional regulator), and the manganese transporters MntT and MtsAB (37, 41). In the CFTR expression cells these proteins were not changed, up-regulated to a lesser extent, or downregulated, resulting in an apparent strong down-regulation when comparing the CFTR expression cells with the control cells (Fig. 6, upper row, patterns #2, 4 or 5). This finding suggests that in the late-exponential and stationary growth phases *L. lactis* normally up-regulates the proteins involved in oxidative stress, even in the absence of excess oxygen (the cultures were grown semi-anaerobically), but that this response is largely absent in the CFTR expression cells.

To sum up, multiple stress responses were observed in *L. lactis* upon CFTR expression, the most obvious of which are the responses to heat shock (misfolded protein) and cell envelope stress. Similar responses to the expression of (nonnative) proteins have also been observed in other organisms (e.g. *E. coli* or *Bacillus subtilis* (42, 43)). The stress experienced by *L. lactis* could be related directly to the presence of CFTR, i.e. CFTR misfolds, and the misfolded protein affects

the integrity of the membrane leading to cell envelope stress. Alternatively, the stress responses may be an indirect consequence of CFTR production, similar to the cellular responses that have been observed in *E. coli* as a consequence of membrane protein overexpression. Overexpression of membrane proteins in *E. coli* caused overloading of the membrane proteins insertion machinery (the Sec machinery), resulting in misfolding/aggregation of endogenous proteins targeted for secretion (42). To distinguish between the two possibilities, we examined the effects of CFTR expression on the translation and targeting and membrane insertion machinery.

Translation and Targeting—The majority of integral membrane proteins are targeted to the Sec translocase as ribosome-bound nascent chains, which are cotranslationally inserted into the membrane upon docking on the Sec translocon (44–46). Higher rates of membrane protein translation may result in a higher fraction of ribosomes associated with the membrane (47), e.g. induced synthesis of bacteriorhodopsin increases the amounts of ribosomes isolated with the membrane fraction (48). In *E. coli* an increased fraction of membrane bound ribosomes caused by membrane protein overexpression resulted in overloading of the Sec insertion machinery, and consequently toxicity to the cell (42). In *L. lactis* the situation is very different: The abundance of ribosomal proteins in the membrane fraction decreased as a function of time in both the control cells and in the CFTR-expressing cells, albeit at different pace (Fig. 5B). Also in the soluble fraction the amounts of ribosomal proteins went down in time, both in the control and CFTR-expressing cells (Fig. 5B). Thus, the absolute amounts of ribosomes decreased, both in the control and in the CFTR expression cells, and both in the membrane and in the soluble fractions. In contrast, the abundance of translocon channel SecY, as well as SecA, the motor protein for protein secretion, remained unchanged in the membrane fraction. As the majority of integral membrane proteins are targeted to the Sec translocase as ribosome-bound nascent chain/Ffh/FtsY complex (49), this result indicates that it is very unlikely that the Sec translocon became overloaded in *L. lactis* upon CFTR expression. The unchanged level of SecY in itself also points at the absence of jammed translocons, because jammed translocons are degraded rapidly (50). Therefore, we tentatively conclude that the misfolded protein response is not triggered by secondary effects (Sec overloading), but rather directly by CFTR expression.

When the abundances of ribosomal protein were compared *between* the control and expression cells at the 1 and 4 h time point, we found that many ribosomal proteins had apparently increased in abundance in the membrane fraction of the CFTR expressing cells compared with the control cells whereas their levels in the soluble fraction remained unchanged (Fig. 5B). The apparent up-regulation of ribosomal proteins in the membrane fraction was caused by a stronger down-regulation in the control cells in comparison to the CFTR-expressing cells (Fig. 6, top row, pattern #4), and the unchanged levels of

ribosomal proteins in the soluble fraction resulted from their down-regulation in the control and CFTR-expressing cells to the same extent (Fig. 6, middle row, pattern #2). Statistical analysis using iterative Group Analysis (iGA, (30)) confirmed that almost all ribosomal subunits cluster among the proteins with the highest iTRAQ ratios in the membrane fraction but not in the soluble fraction. These results show that the distribution of ribosomes over the membrane and soluble fractions becomes different in the control and CFTR expressing cells as a function of induction time. The redistribution takes place predominantly in the control cells, where the fraction of membrane bound ribosomes decreases to a much larger extent than in soluble fraction. In the CFTR-expressing cells the distribution remains approximately the same. This finding is surprising, and shows that normal (control) *L. lactis* cells entering the late exponential or stationary growth phase specifically decrease the amounts of membrane bound ribosomes, perhaps indicating a lower need for integral membrane and secreted proteins.

The signal recognition particle protein Ffh increased in abundance at the membrane on CFTR expression. Because the receptor FtsY remained unchanged, and membrane associated ribosomal proteins decreased upon expression, a possible explanation for the increased Ffh abundance is that the ribosome-nascent chain complexes stayed attached for longer with the signal recognition particle after targeting to the membrane. Increased association times at the membrane could be indicative of hindered translation, in which case the ribosomes, mRNA and other components of the translation machinery have to be recycled from the stalled ribosomes. In particular peptidyl-tRNAs must be degraded because they are toxic to the cell (51, 52). Several proteins involved in ribosome recycling, including Pth (peptidyl tRNA hydrolase), Frr (ribosomal recycling factor), InfC (initiation factor), and RelA (GTP pyrophosphokinase), increased in abundance upon CFTR expression (53–58). We therefore tentatively conclude that CFTR expression leads to a higher extent of stalled ribosomes, which necessitates their rescue.

Ribosomal biogenesis was reduced when comparing the CFTR expressing cells with the control cells (Fig. 6, top row, pattern #5), as indicated by apparent down-regulation of almost all polypeptides of the ribosomal RNA methyltransferase, the ribosomal biogenesis GTPases Era and Iimg_1175, the ribosome maturation factor RimM and the ribonuclease Rnc, which is involved into rRNA processing together with the ribosome maturation factor RimM (59–61). The apparent reduction of ribosome biogenesis correlates with the observed growth stasis (Fig. 7).

Metabolism

Nitrogen Metabolism—CFTR expression strongly affected nitrogen metabolism. CodY is a global repressor of genes that become expressed only when nitrogen sources are limiting

(62, 63). Proteins of which the expression is regulated by CodY were collectively lower in abundance in the CFTR expression strain than in the control strain, indicative of higher intracellular levels of branched-chain amino acids (corepressors of CodY) and presumably higher levels of amino acids in general. Among the proteins with the strongest down-regulation were the subunits of the oligopeptide transport system Opp (Fig. 5A), the peptidase PepO, enzymes of the branched-chain amino acid synthetic pathway (IlvC, IlvE), glutamate synthase GltBD, the branched chain amino acid transporter CtrA, and asparagine synthase AsnB. Without exception, the apparent down-regulation of these proteins was caused by strong up-regulation in the control cells, which did not occur in the CFTR expressing cells (Fig. 6, upper row, patterns #4 and #5, see also Fig. 5A for the Opp proteins). Also other proteins regulated by nitrogen limitation were apparently down-regulated, such as the nitrogen regulatory protein GlnB (P-II), the glutamine synthetase regulator GlnR, glutamine synthetase GlnA, the di- and tripeptide transporter DtpT, and the numerous peptidases involved in the breakdown of imported peptides (PepA, PepT, PepO2, PepN, PepP, PepDA, and PepDB). The data indicates that the control cells become starved for nitrogen at timepoints 1 h and 4 h, but that the CFTR expressing cells experience no shortage of nitrogen supply. This is consistent with the fast growth of the control cells (supplemental Fig. 1), which deplete the available nitrogen compounds for biomass production, and the growth arrest of the CFTR expressing cells, which lowers the need for nitrogen compounds. It is remarkable that the strong up-regulation in the control cells is noticeable already after 1 h of induction when the cells still appear to be growing exponentially (albeit in the late exponential phase). Clearly *L. lactis* begins to experience nitrogen shortage in this phase already.

Sugar Metabolism—The effects of CFTR expression on the sugar metabolism are not as clear-cut as in the case of the nitrogen metabolism, possibly because many of the enzymes involved in glycolysis, and pathways downstream of pyruvate are not primarily regulated at the level of expression, but rather by allosteric and feedback regulation using molecules that sample the energetic status (such as the NADH/NAD⁺ and ADT/ADP ratio). Nonetheless there are indications that the control cells become starved for sugar, as opposed to the CFTR expression cells. For example, the PTS transport systems for alternative sugars (cellobiose and mannose) become more abundant as function of time in the control cells, but not in the expression cells. Similarly, AdhE (alcohol acetaldehyde dehydrogenase) increases in abundance in the control cells only, indicating that these cells are switching to mixed acid fermentation to produce more ATP. Shortage of ATP is also indicated by up-regulation of the F-type ATPase in the control cells only.

Taken together the data indicates that the direct effects of CFTR expression on metabolism are minor. The main difference between the control cells and the expression cells is that

the control cells continue to grow rapidly after induction, thereby depleting their sugar and nitrogen supplies, whereas the expressing cells stop growing, and, initially, do not experience energy and nitrogen shortage. In *E. coli* the situation is very different: Upon overexpression of membrane proteins the Sec translocon becomes overloaded, which negatively affects the levels of respiratory enzymes in the membrane, and leads to activation of the Arc two-component system, which mediates adaptive responses to changing respiratory states. The acetate-phosphotransacetylase pathway for ATP production was induced and the tricarboxylic acid cycle was down-regulated. *E. coli* thus switches to a less efficient energy metabolism, which strongly affects biomass production (42).

Outlook—The different responses of *E. coli* and *L. lactis* to stress caused by membrane protein expression imply that different strategies must be used to remedy expression bottlenecks. In *E. coli*, careful tuning of the expression levels (to prevent overloading of the Sec machinery) has been used successfully to optimize expression levels (64). What can be done to improve the expression of CFTR in *L. lactis*? The answer hinges on two possibilities. 1) It is possible that CFTR was folded properly upon expression in *L. lactis*, but that the protein was recognized as a misfolded protein (because it is non-endogenous). In that case the answer could be to trick *L. lactis* and force it not to use the stress responses and thus to prevent growth arrest, e.g. by deleting heat shock proteins (65). 2) If CFTR was not properly folded, then the protein could be helped to fold properly, e.g. by including (human) chaperones, or by mutagenesis, such as changing all the phosphorylation sites in the R-domain into negatively charged residues. Chaperone co-expression has been used with mixed success to improve heterologous expression in *E. coli* (66–68). Also, the production of recombinant proteins under thermal stress could be improved by co-expression of GroESL in *E. coli* (69). The fact that the expression of CFTR improved at higher temperatures (supplemental Fig. S3) indeed suggests that the up-regulation of heat shock proteins helps *L. lactis* to deal better with the expression stress. Again, this is very different from what is normally observed in *E. coli*, where lower temperatures, and thus lower expression rates, usually improve production, possibly because overloading of the Sec machinery is prevented.

Acknowledgments—We thank Peter Maloney (Johns Hopkins Medical School), Mohabir Ramjeesingh (University of Toronto) and Bert Poolman (University of Groningen) for their helpful comments.

* This work was supported by the Netherlands Organisation for Scientific Research NWO (VIDI fellowships to DJS and RB), the Netherlands Proteomics Centre (NPC), the Cystic Fibrosis Foundation Therapeutics, Inc. (CFFT), the European Union (EDICT program), the EFRO (Europees Fonds voor Regionale Ontwikkeling) and the Province of Groningen (IAG-2).

§ This article contains supplemental Figs. S1 to S3 and Tables S1 to S6.

¶ To whom correspondence should be addressed: Department of Biochemistry Groningen Biomolecular Sciences and Biotechnology Institute, University of Groningen, Nijenborgh 4, 9747 AG, Groningen, The Netherlands. Tel.: 0031-50-3634187; Fax: 0031-50-3634165; E-mail: d.j.slotboom@rug.nl.

|| Shared first authors.

REFERENCES

1. Rommens, J. M., Iannuzzi, M. C., Kerem, B., Drumm, M. L., Melmer, G., Dean, M., Rozmahel, R., Cole, J. L., Kennedy, D., Hidaka, N., Zsiga, M., Buchwald, M., Riordan, J. R., Lap, C. T., and Collins, F. S. (1989) Identification of the cystic fibrosis gene: chromosome walking and jumping. *Science* **245**, 1059–1065
2. Kerem, B., Rommens, J. M., Buchanan, J. A., Markiewicz, D., Cox, T. K., Chakravarti, A., Buchwald, M., and Tsui, L. C. (1989) Identification of the cystic fibrosis gene: genetic analysis. *Science* **245**, 1073–1080
3. Riordan, J. R., Rommens, J. M., Kerem, B., Alon, N., Rozmahel, R., Grzelczak, Z., Zielenski, J., Lok, S., Plavsic, N., Chou, J. L., et al. (1989) Identification of the cystic fibrosis gene: cloning and characterization of complementary DNA. *Science* **245**, 1066–1073
4. Surade, S., Klein, M., Stolt-Bergner, P. C., Muenke, C., Roy, A., and Michel, H. (2006) Comparative analysis and “expression space” coverage of the production of prokaryotic membrane proteins for structural genomics. *Protein Sci.* **15**, 2178–2189
5. Kunji, E. R., Slotboom, D. J., and Poolman, B. (2003) *Lactococcus lactis* as host for overproduction of functional membrane proteins. *Biochim. Biophys. Acta.* **1610**, 97–108
6. Tate, C. G., Haase, J., Baker, C., Boersma, M., Magnani, F., Vallis, Y., and Williams, D. C. (2003) Comparison of seven different heterologous protein expression systems for the production of the serotonin transporter. *Biochim. Biophys. Acta* **1610**, 141–153
7. Tate, C. G., and Grishammer, R. (1996) Heterologous expression of G-protein-coupled receptors. *Trends Biotechnol.* **14**, 426–430
8. Grishammer, R., and Tate, C. G. (1995) Overexpression of integral membrane proteins for structural studies. *Q. Rev. Biophys.* **28**, 315–422
9. Cereghino, J. L., and Cregg, J. M. (2000) Heterologous protein expression in the methylotrophic yeast *Pichia pastoris*. *FEMS Microbiol. Rev.* **24**, 45–66
10. Bonander, N., and Bill, R. M. (2009) Relieving the first bottleneck in the drug discovery pipeline: using array technologies to rationalize membrane protein production. *Expert Rev. Proteomics* **6**, 501–505
11. Zweers, J. C., Wiegert, T., and van Dijk, J. M. (2009) Stress-responsive systems set specific limits to the overproduction of membrane proteins in *Bacillus subtilis*. *Appl. Environ. Microbiol.* **75**, 7356–7364
12. de Ruyter, P. G., Kuipers, O. P., and de Vos, W. M. (1996) Controlled gene expression systems for *Lactococcus lactis* with the food-grade inducer nisin. *Appl. Environ. Microbiol.* **62**, 3662–3667
13. Frelet-Barrand, A., Boutigny, S., Moyet, L., Deniaud, A., Seigneurin-Berny, D., Salvi, D., Bernaudat, F., Richaud, P., Pebay-Peyroula, E., Joyard, J., and Rolland, N. *Lactococcus lactis*, an alternative system for functional expression of peripheral and intrinsic Arabidopsis membrane proteins. *PLoS One* **5**, e8746
14. Kunji, E. R., Chan, K. W., Slotboom, D. J., Floyd, S., O’Connor, R., and Monné, M. (2005) Eukaryotic membrane protein overproduction in *Lactococcus lactis*. *Curr. Opin. Biotechnol.* **16**, 546–551
15. Monné, M., Chan, K. W., Slotboom, D. J., and Kunji, E. R. (2005) Functional expression of eukaryotic membrane proteins in *Lactococcus lactis*. *Protein Sci.* **14**, 3048–3056
16. Monné, M., Robinson, A. J., Boes, C., Harbour, M. E., Fearnley, I. M., and Kunji, E. R. (2007) The mimivirus genome encodes a mitochondrial carrier that transports dATP and dTTP. *J. Virol.* **81**, 3181–3186
17. Quick, M., and Javitch, J. A. (2007) Monitoring the function of membrane transport proteins in detergent-solubilized form. *Proc. Natl. Acad. Sci. U.S.A.* **104**, 3603–3608
18. Luirink, J., Samuelsson, T., and de Gier, J. W. (2001) YidC/Oxa1p/Alb3: evolutionarily conserved mediators of membrane protein assembly. *FEBS Lett.* **501**, 1–5
19. Zweers, J. C., Barák, I., Becher, D., Driessen, A. J., Hecker, M., Kontinen, V. P., Saller, M. J., Vavrová, L., and van, Dijk, J. M. (2008) Towards the development of *Bacillus subtilis* as a cell factory for membrane proteins

- and protein complexes. *Microb. Cell Fact.* **7**, 10
20. Funes, S., Hasona, A., Bauerschmitt, H., Grubbauer, C., Kauff, F., Collins, R., Crowley, P. J., Palmer, S. R., Brady, L. J., and Herrmann, J. M. (2009) Independent gene duplications of the YidC/Oxa/Alb3 family enabled a specialized cotranslational function. *Proc. Natl. Acad. Sci. U.S.A.* **106**, 6656–6661
 21. Geertsma, E. R., and Poolman, B. (2007) High-throughput cloning and expression in recalcitrant bacteria. *Nat. Methods* **4**, 705–707
 22. Keller, A., Nesvizhskii, A. I., Kolker, E., and Aebersold, R. (2002) Empirical statistical model to estimate the accuracy of peptide identifications made by MS/MS and database search. *Anal. Chem.* **74**, 5383–5392
 23. Nesvizhskii, A. I., Keller, A., Kolker, E., and Aebersold, R. (2003) A statistical model for identifying proteins by tandem mass spectrometry. *Anal. Chem.* **75**, 4646–4658
 24. Breitling, R., Armengaud, P., Amtmann, A., and Herzyk, P. (2004) Rank products: a simple, yet powerful, new method to detect differentially regulated genes in replicated microarray experiments. *FEBS Letts.* **573**, 83–92
 25. Breitling, R., and Herzyk, P. (2005) Rank-based methods as a non-parametric alternative of the T-statistic for the analysis of biological microarray data. *J. Bioinform. Comput. Biol.* **3**, 1171–1189
 26. Hong, F., Breitling, R., McEntee, C. W., Wittner, B. S., Nemhauser, J. L., and Chory, J. (2006) RankProd: a bioconductor package for detecting differentially expressed genes in meta-analysis. *Bioinformatics* **22**, 2825–2827
 27. Benjamini, Y., and Hochberg, Y. (2000) On the adaptive control of the false discovery rate in multiple testing with independent statistics. *J. Educ. Behav. Stat.* **25**, 60–83
 28. Strimmer, K. (2008) fdrtool: a versatile R package for estimating local and tail area-based false discovery rates. *Bioinformatics* **24**, 1461–1462
 29. Breitling, R., Amtmann, A., and Herzyk, P. (2004) Iterative Group Analysis (iGA): A simple tool to enhance sensitivity and facilitate interpretation of microarray experiments. *BMC Bioinformatics* **5**, 34
 30. Wiederhold, E., Gandhi, T., Permentier, H. P., Breitling, R., Poolman, B., and Slotboom, D. J. (2009) The yeast vacuolar membrane proteome. *Mol. Cell. Proteomics* **8**, 380–392
 31. Drumm, M. L., Pope, H. A., Cliff, W. H., Rommens, J. M., Marvin, S. A., Tsui, L. C., Collins, F. S., Frizzell, R. A., and Wilson, J. M. (1990) Correction of the cystic fibrosis defect in vitro by retrovirus-mediated gene transfer. *Cell* **62**, 1227–1233
 32. Gregory, R. J., Cheng, S. H., Rich, D. P., Marshall, J., Paul, S., Hehir, K., Ostedgaard, L., Klinger, K. W., Welsh, M. J., and Smith, A. E. (1990) Expression and characterization of the cystic fibrosis transmembrane conductance regulator. *Nature* **347**, 382–386
 33. Ow, S. Y., Salim, M., Noirel, J., Evans, C., Rehman, I., and Wright, P. C. (2009) iTRAQ underestimation in simple and complex mixtures: “the good, the bad and the ugly”. *J. Proteome Res.* **8**, 5347–5355
 34. Berkelman, T., Garret-Engel, P., and Hoffman, N. E. (1994) The *pacL* gene of *Synechococcus* sp. strain PCC 7942 encodes a $Ca(2+)$ -transporting ATPase. *J. Bacteriol.* **176**, 4430–4436
 35. Martínez, B., Zomer, A. L., Rodríguez, A., Kok, J., and Kuipers, O. P. (2007) Cell envelope stress induced by the bacteriocin Lcn972 is sensed by the Lactococcal two-component system CesSR. *Mol. Microbiol.* **64**, 473–486
 36. Rocas, C., Campelo, A. B., Veiga, P., Pinto, J. P., Rodríguez, A., and Martínez, B. (2009) Contribution of the CesR-regulated genes *llmg0169* and *llmg2164–2163* to *Lactococcus lactis* fitness. *Int. J. Food Microbiol.* **133**, 279–285
 37. van de Guchte, M., Serror, P., Chervaux, C., Smokvina, T., Ehrlich, S. D., and Maguin, E. (2002) Stress responses in lactic acid bacteria. *Antonie Van Leeuwenhoek* **82**, 187–216
 38. Ingmer, H., Vogensen, F. K., Hammer, K., and Kilstrup, M. (1999) Disruption and Analysis of the *clpB*, *clpC*, and *clpE* Genes in *Lactococcus lactis*: ClpE, a New Clp Family in Gram-Positive Bacteria. *J. Bacteriol.* **181**, 2075–2083
 39. Prieto-Alamo, M. J., Jurado, J., Gallardo-Madueno, R., Monje-Casas, F., Holmgren, A., and Pueyo, C. (2000) Transcriptional regulation of glutaredoxin and thioredoxin pathways and related enzymes in response to oxidative stress. *J. Biol. Chem.* **275**, 13398–13405
 40. Jobin, M. P., Garmyn, D., Diviès, C., and Guzzo, J. (1999) Expression of the *Oenococcus oeni* *trxA* gene is induced by hydrogen peroxide and heat shock. *Microbiology* **145**, 1245–1251
 41. Miyoshi, A., Rochat, T., Gratadoux, J. J., Le Loir, Y., Oliveira, S. C., Langella, P., and Azevedo, V. (2003) Oxidative stress in *Lactococcus lactis*. *Gen. Mol. Res.* **2**, 348–359
 42. Wagner, S., Baars, L., Ytterberg, A. J., Klussmeier, A., Wagner, C. S., Nord, O., Nygren, P. A., van Wijk, K. J., and de Gier, J. W. (2007) Consequences of membrane protein overexpression in *Escherichia coli*. *Mol. Cell. Proteomics* **6**, 1527–1550
 43. Mogk, A., Völker, A., Engelmann, S., Hecker, M., Schumann, W., and Völker, U. (1998) Nonnative Proteins Induce Expression of the *Bacillus subtilis* CIRCE Regulon. *J. Bacteriol.* **180**, 2895–2900
 44. Valent, Q. A., Scotti, P. A., High, S., de Gier, J. W., von Heijne, G., Lentzen, G., Wintermeyer, W., Oudega, B., and Lührink, J. (1998) The *Escherichia coli* SRP and SecB targeting pathways converge at the translocon. *EMBO J.* **17**, 2504–2512
 45. de Gier, J. W., and Lührink, J. (2001) Biogenesis of inner membrane proteins in *Escherichia coli*. *Mol. Microbiol.* **40**, 314–322
 46. Urbanus, M. L., Scotti, P. A., Froderberg, L., Saaf, A., de Gier, J. W., Brunner, J., Samuelson, J. C., Dalbey, R. E., Oudega, B., and Lührink, J. (2001) Sec-dependent membrane protein insertion: sequential interaction of nascent FtsQ with SecY and YidC. *EMBO Rep.* **2**, 524–529
 47. Bisle, B., Schmidt, A., Scheibe, B., Klein, C., Tebbe, A., Kellermann, J., Siedler, F., Pfeiffer, F., Lottspeich, F., and Oesterhelt, D. (2006) Quantitative Profiling of the Membrane Proteome in a Halophilic Archaeon. *Mol. Cell. Proteomics* **5**, 1543–1558
 48. Gropp, R., Gropp, F., and Betlach, M. C. (1992) Association of the halobacterial 7S RNA to the polysome correlates with expression of the membrane protein bacterioopsin. *Proc. Natl. Acad. Sci. U.S.A.* **89**, 1204–1208
 49. Lührink, J., von Heijne, G., Houben, E., and de Gier, J. W. (2005) Biogenesis of Inner Membrane Proteins in *Escherichia coli*. *Ann. Rev. Microbiol.* **59**, 329–355
 50. van Stelten, J., Silva, F., Belin, D., and Silhavy, T. J. (2009) Effects of antibiotics and a proto-oncogene homolog on destruction of protein translocator SecY. *Science* **325**, 753–756
 51. Menninger, J. R. (1979) Accumulation of peptidyl tRNA is lethal to *Escherichia coli*. *J. Bacteriol.* **137**, 694–696
 52. Atherly, A. G., and Menninger, J. R. (1972) Mutant *E. coli* strain with temperature sensitive peptidyl-transfer RNA hydrolase. *Nat. New Biol.* **240**, 245–246
 53. Heurgué-Hamard, V., Karimi, R., Mora, L., MacDougall, J., Leboeuf, C., Grenzmann, G., Ehrenberg, M., and Buckingham, R. H. (1998) Ribosome release factor RF4 and termination factor RF3 are involved in dissociation of peptidyl-tRNA from the ribosome. *EMBO J.* **17**, 808–816
 54. Karimi, R., Pavlov, M. Y., Heurgué-Hamard, V., Buckingham, R. H., and Ehrenberg, M. (1998) Initiation factors IF1 and IF2 synergistically remove peptidyl-tRNAs with short polypeptides from the P-site of translating *Escherichia coli* ribosomes. *J. Mol. Biol.* **281**, 241–252
 55. Menninger, J. R., Caplan, A. B., Gingrich, P. K., and Atherly, A. G. (1983) Tests of the ribosome editor hypothesis. II. Relaxed (*relA*) and stringent (*relA+*) *E. coli* differ in rates of dissociation of peptidyl-tRNA from ribosomes. *Mol. Gen. Genet.* **190**, 215–221
 56. Rao, A. R., and Varshney, U. (2001) Specific interaction between the ribosome recycling factor and the elongation factor G from *Mycobacterium tuberculosis* mediates peptidyl-tRNA release and ribosome recycling in *Escherichia coli*. *EMBO J.* **20**, 2977–2986
 57. Kossel, H., and RajBhandary, U. L. (1968) Studies on polynucleotides. LXXXVI. Enzymic hydrolysis of N-acylaminoacyl-transfer RNA. *J. Mol. Biol.* **35**, 539–560
 58. Singh, N. S., and Varshney, U. (2004) A physiological connection between tmRNA and peptidyl-tRNA hydrolase functions in *Escherichia coli*. *Nucleic Acids Res.* **32**, 6028–6037
 59. Comartin, D. J., and Brown, E. D. (2006) Non-ribosomal factors in ribosome subunit assembly are emerging targets for new antibacterial drugs. *Curr. Opin. Pharmacol.* **6**, 453–458
 60. Dunn, J. J., and Studier, F. W. (1973) T7 early RNAs and *Escherichia coli* ribosomal RNAs are cut from large precursor RNAs in vivo by ribonuclease 3. *Proc. Natl. Acad. Sci. U.S.A.* **70**, 3296–3300
 61. Drider, D., Bolotine, A., Renault, P., and Prevost, H. (2002) Functional study of *Lactococcus lactis* RNase III in *Escherichia coli*. *Plasmid* **47**, 246–250
 62. den Hengst, C. D., van Hijum, S. A., Geurts, J. M., Nauta, A., Kok, J., and Kuipers, O. P. (2005) The *Lactococcus lactis* CodY Regulon: Identifica-

- tion of A Conserved Cis-Regulatory Element. *J. Biol. Chem.* **280**, 34332–34342
63. Guédon, E., Sperandio, B., Pons, N., Ehrlich, S. D., and Renault, P. (2005) Overall control of nitrogen metabolism in *Lactococcus lactis* by CodY, and possible models for CodY regulation in Firmicutes. *Microbiology* **151**, 3895–3909
64. Wagner, S., Klepsch, M. M., Schlegel, S., Appel, A., Draheim, R., Tarry, M., Högbom, M., van Wijk, K. J., Slotboom, D. J., Persson, J. O., and de Gier, J. W. (2008) Tuning *Escherichia coli* for membrane protein overexpression. *Proc. Natl. Acad. Sci. U.S.A.* **105**, 14371–14376
65. Skretas, G., and Georgiou, G. (2009) Genetic analysis of G protein-coupled receptor expression in *Escherichia coli*: inhibitory role of DnaJ on the membrane integration of the human central cannabinoid receptor. *Bio-technol. Bioeng.* **102**, 357–367
66. Chen, Y., Song, J., Sui, S. F., and Wang, D. N. (2003) DnaK and DnaJ facilitated the folding process and reduced inclusion body formation of magnesium transporter CorA overexpressed in *Escherichia coli*. *Protein Exp. Purif.* **32**, 221–231
67. Link, A. J., Skretas, G., Strauch, E. M., Chari, N. S., and Georgiou, G. (2008) Efficient production of membrane-integrated and detergent-soluble G protein-coupled receptors in *Escherichia coli*. *Protein Sci.* **17**, 1857–1863
68. Kolaj, O., Spada, S., Robin, S., and Wall, J. G. (2009) Use of folding modulators to improve heterologous protein production in *Escherichia coli*. *Microbial Cell Factories* **8**, 9–25
69. Kim, S. Y., Ayyadurai, N., Heo, M. A., Park, S., Jeong, Y. J., and Lee, S.G. (2009) Improving the Productivity of Recombinant Protein in *Escherichia coli* Under Thermal Stress by Coexpressing GroELS Chaperone System. *J. Microbiol. Biotechnol.* **19**, 72–77